Shorted Stacked Patch Array for Photonic Beam Steering at mm-Waves

Charikleia Tzimoragka, Ronan Sauleau, Mehdi Alouini, Cyril Paranthoen, David Gonzalez-Ovejero

Shorted Stacked Patch Array for Photonic Beam Steering at mm-Waves

Charikleia Tzimoragka[1,2], Ronan Sauleau[1], Mehdi Alouini[2], Cyril Paranthoen[3], David González-Ovejero[1]
[1]Univ Rennes, CNRS, IETR – UMR 6164, F-35000, Rennes,France
[2]Univ Rennes, CNRS, Institut FOTON – UMR 6082, F-35000 Rennes, France
[3]Univ Rennes, INSA, CNRS, Institut FOTON – UMR 6082, F-35000 Rennes, France
charikleia.tzimoragka@univ-rennes.fr

***Abstract*—We present the design of a mm-wave phased array antenna enabled by photonic beam steering. The mm-wave signal is generated by InP uni-traveling-carrier (UTC) photodiodes within the photonic integrated chip (PIC). The antenna array consists of four sub-arrays, each comprising two stacked patch elements. The bottom patch is shorted to create a compact element, enabling a half-wavelength spacing in the scanning plane. This configuration results in a relatively wide scanning range of +/-30° without significant sidelobe levels. The complexity of this structure lies in the heterogeneous integration of the InP chip with the antenna array and biasing network, all printed on a low-loss substrate with low relative permittivity. The proposed array exhibits a simulated peak directivity of 16 dBi and an impedance and -3 dB gain bandwidth ranging from 43.8 GHz to 58.8 GHz.**

***Index Terms*—beam-steering, phased array, shorted patch, mm-wave, photomixing antenna, wireless communication.**

I. Introduction

Based on recent reports [1], wireless data traffic has significantly increased, almost doubling, since 2021 and is expected to expand by a factor of 3.5 by the end of 2028. The exponentially increasing demand for data and quality requirements pose an important concern about whether the capacity of backhaul links in current access networks will be sufficient [2]. One way to support the rapid growth of data is to adopt carriers in higher frequency bands, which results in larger total bandwidths. Following this trend, millimeter (mm) and sub-millimeter (sub-mm) wave communication systems have experienced a rapid development in the last decade. However, there are still some challenges to be addressed for the widespread use of mm- and sub-mm frequency bands. These challenges include the high free-space path loss that the link must face and the relatively low power generated by room-temperature continuous wave sources [2], [3].

Mm- and sub-mm wave wireless links typically employ either an electronic approach for up-converting millimeter-wave signals or a photonic approach for down-converting from the optical domain. The photonic generation of signals through photomixing is an extremely promising avenue to explore, as the mm-wave signal generated by photomixing transmitters is tunable over a wide bandwidth, and one can take advantage of reliable and cost-effective optical amplifiers (EDFA, SOA), high frequency modulators and integrated photonic circuits. Furthermore, it becomes feasible to establish a seamless connection between sub-THz radio and $1.55\,\mu\mathrm{m}$ data flows guided by optical fibers [4]. Despite unlocking significantly broad bandwidths, mm and sub-mm carriers come with significant propagation losses. However, the use of high-gain antennas with beam-steering capabilities can mitigate misalignment losses and maximize the amount of power transmitted in the receiver's direction [5], [6].

This paper presents a phased array architecture using low-cost single-layer PCB technology for heterogeneous integration with a photonic integrated circuit (PIC), which provides the phase shifting and mm-wave signal generation functionalities by uni-traveling-carrier photodiodes (UTC-PDs). However, using a single layer comes with some challenges, such as accommodating the feed network and mitigating mutual coupling in a closely packed array, which is necessary for relatively wide beam scanning. Additionally, one must include the lines to bias the UTC-PDs in the PIC. The proposed compact antenna element [7] allows one to reduce the distance between the subarrays to $0.5 \times \lambda_0$, with λ_0 being the free space wavelength, which leads to a wide scanning angle of $\pm 30°$ with 15 GHz impedance bandwidth from 43.8 GHz to 58.8 GHz and a -3 dB gain bandwidth through the band of interest.

This paper is organized as follows. The overall architecture for photonic-enabled beam-steering is succinctly described in Section II. Section III describes the structure of the shorted stacked patch phased array. The simulated results about the beam-switching capabilities and the directivity of the total phased array are discussed in Section IV. Finally, conclusions and future perspectives are discussed in Section V.

II. Photonically achieved Beam Steering

In high-frequency wireless communication, the transmitter architecture leverages photonic technology to generate the transmitted signal and achieve beam steering. This approach capitalizes on cost-effective photonic components for signal amplification and facilitates the attainment of high modulation speeds. Fig. 1 depicts, the planned transmitter architecture, starting with the use of a dual-frequency laser within the telecommunication optical C-Band. This laser is employed to generate two closely correlated wavelengths [8], where

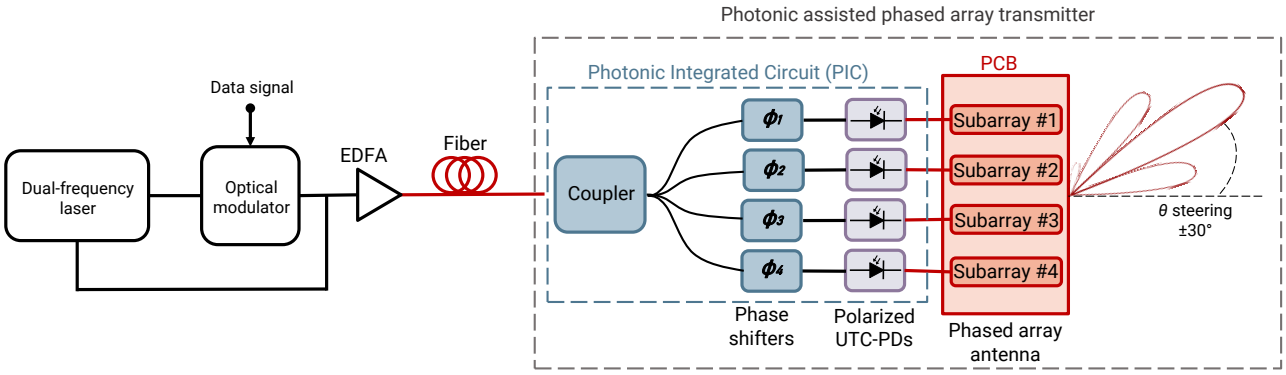

Fig. 1. Schematic of the emission structure

frequency stabilization is possible on each wavelength independently [9]. Subsequently, one of these optical carriers undergoes modulation in both phase and amplitude through a photonic IQ modulator, according to an M-QAM modulation format. Following, an Erbium Doped Fiber Amplifier (EDFA) is introduced with an optical filter in order to amplify the signal without facing spontaneous emission noise caused by the amplifier. Then the structure is split into four branches, followed by phase-shifters to the UTC-PDs which are connected to each sub-array. UTC-PDs illuminated at 1550 nm optical window, are observed to demonstrate significantly reduced signal losses and achieve a higher output power than photoconductors illuminated at 800 nm [10].

III. Antenna Design

This section presents the structure and the assembly strategy for the phased array for operation at a center frequency of 51.5 GHz. Fig. 2 shows the geometry of the structure at hand.

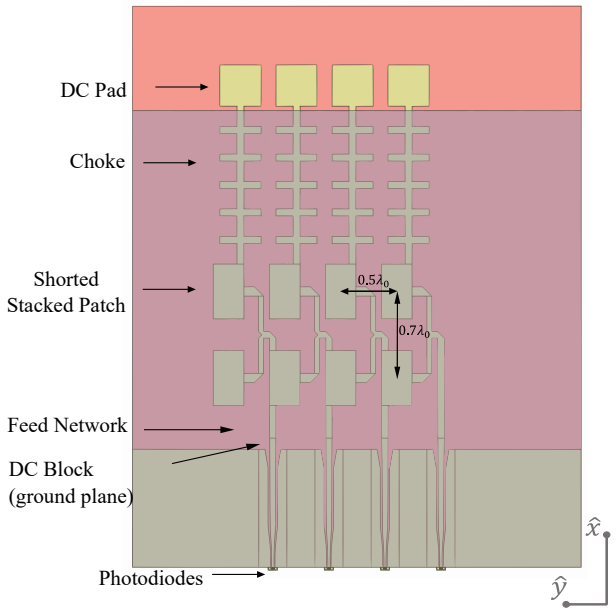

Fig. 2. Phased Array architecture with the different sections indicated.

The array consists of 4 column sub-arrays, each excited by a UTC-PD on an InP platform. The array is compatible with single-layer PCB technology, using a grounded RT/Duroid™ 5880 laminate with thickness 252 µm, $\varepsilon_r = 2.2$ and dielectric losses given by $\tan\delta = 0.009$.

A. Shorted Stacked Patch

Each sub-array consists of two shorted stacked patches separated by a distance of $0.7 \times \lambda_0$. The structure of the shorted stacked patch is shown in Fig. 3. It is composed of one patch with thickness $t_p = 30\,\mu\text{m}$ printed on a grounded dielectric layer of RT/Duroid™ 5880 ($\varepsilon_r = 2.2$, $\tan\delta = 0.009$) with thickness $t_{\text{sub}} = 252\,\mu\text{m}$. The radiating patch is shorted with two vias, each with a diameter $d_{\text{vias}} = 320\,\mu\text{m}$ and is fed by a $50\,\Omega$ microstrip line with a width of $W_m = 500\,\mu\text{m}$. The length of the shorted patch is $L_p = 1000\,\mu\text{m}$ and the width $W_p = 2940\,\mu\text{m}$. A parasitic patch is positioned, with air gap, at a height of $h_{\text{gap}} = 388\,\mu\text{m}$ above the shorted patch and is printed on a Quartz Glass superstrate ($\varepsilon_r = 3.78$, $t_{\text{sup}} = 110\,\mu\text{m}$ thickness).

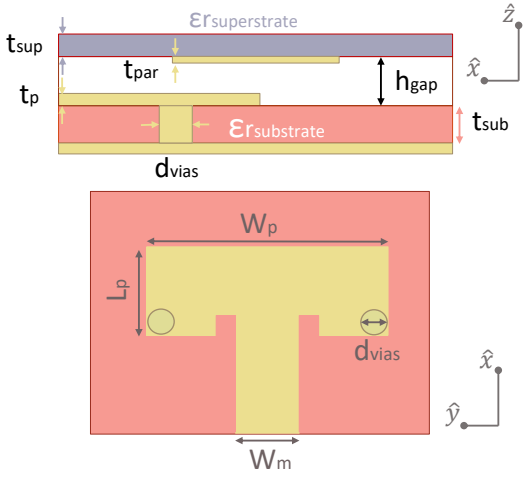

Fig. 3. Detailed view of the shorted stacked patch geometry.

Due to the compact size of the shorted patch, a spacing of $0.5 \times \lambda_0$ can be set between the sub-arrays while keeping the feed network in the same layer. This arrangement allows for scanning to wider angles while preventing the onset of grating lobes.

B. RF-Choke and DC-Bias

Since our sub-arrays are excited with photodiodes, a network is required to bias the photodiodes. Consequently, it becomes essential to incorporate an RF choke and a DC Block. In the current structure, each sub-array is terminated with an RF choke to isolate the surface currents and to separate the radiating portion from the DC pads. The RF choke is designed using microstrip technology and demonstrates simulated RF isolation exceeding 30 dB across the operating frequency range of the array (43.8 GHz to 58.8 GHz). It comprises five consecutive identical parts [11]. Each part consists of a T-shaped structure, with the horizontal bar comprising two shunt open-ended stubs, each a quarter-wavelength ($\lambda/4$) long, effectively creating a short circuit and functioning as an RF choke. Furthermore, the length of the vertical bar in the T-shape is carefully selected to transform the shorted microstrip into a substantial inductive load, resulting in a high input impedance.

On the other hand, a DC block is introduced on the ground plane as shown in Fig. 4 to have a different potential between the signal line and the ground of the co-planar waveguide (CPW), allowing for biasing and monitoring the current of the PDs. The DC Block is designed based on a slotline on the ground plane [12], [13]. It is positioned on the ground plane between the end of the microstrip line and the beginning of the CPW, as depicted in Fig. 2.

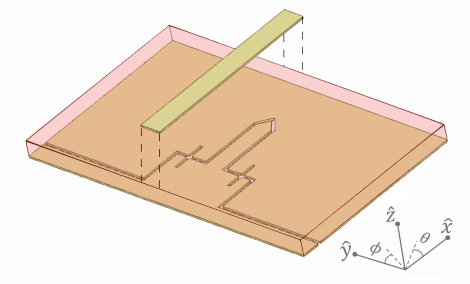

Fig. 4. DC Block placed on the ground plane to seperate the signal from the CPW feeding the PDs.

C. Phased Array

The general assembly of the phased array is depicted in Fig. 2. The shorted patches and the RF-chokes have been arranged as it was described previously. The feeding network is designed with the help of a CPW in order to match the impedance of the photodiodes (PDs). The UTC-PDs [14] are fabricated on InP substrate ($\varepsilon_r = 12.5$) at III-V Lab, integrated with a $50\,\Omega$ grounded co-planar waveguide (G-CPW) and is connected at the end of the transition line.

There are different ways to succeed the heterogeneous integration of the PCB with the InP chip. Wire bonding and thread bonding are crucial methods for establishing electrical connections between InP chips and PCBs. In this structure a similar procedure will be followed as has been described in [11]. First the G-CPW of the InP chip will be aligned to the G-CPW of the PCB. Once both parts are secured, the next step is to bond the UTC-PDs to the G-CPW line on the PCB using a silver epoxy glue. It's important to note that when calculating total losses, the $50\,\Omega$ CPW output of the UTC-photodiodes should be considered, and it doesn't compensate for the photodiode's inherent high reactive component.

In photomixing arrays with a substantial number of photodiodes, simultaneously aligning all the optical fibers with the individual chips is a challenging task. This difficulty arises because coordinating the precise alignment of numerous optical fibers with a correspondingly large number of photodiodes can be a complex and demanding process.

IV. Results - Radiation Patterns

With the current geometry, a 15 GHz impedance bandwidth has been achieved from 43.8 GHz to 58.8 GHz for active reflection coefficient $S_{11} < -10$ dB as it is shown in Fig. 5.

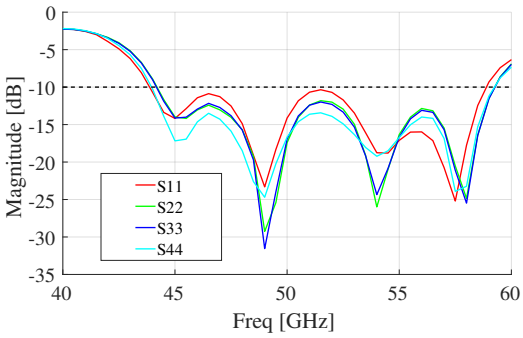

Fig. 5. Simulated magnitude of the input active reflection coefficients in dB.

The total directivity of the whole array, for different scanning angles (0°, 15° and 30°), is displayed in Fig. 6 with a -3 dB gain bandwidth across the desired frequency range.

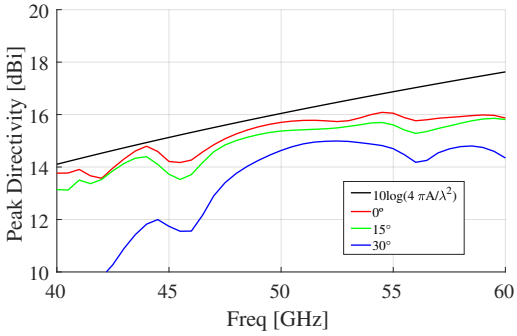

Fig. 6. Directivity of the total array at broadside for 0°, 15° and 30° scanning angle.

Fig. 7 depicts the normalized radiation pattern at 51.5 GHz corresponding to the central frequency within the operating bandwidth.

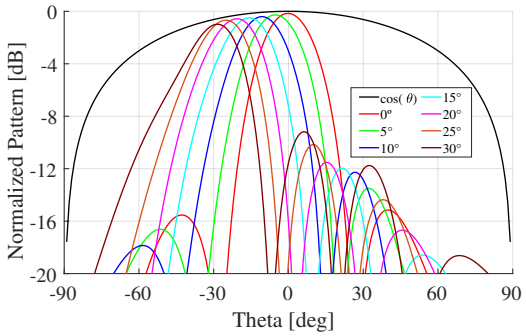

Fig. 7. Radiation Pattern simulated at $\pm 30°$ deflection angle at central frequency 51.5 GHz.

One can observe that a beam steering of $\pm 30°$ is possible throughout the whole frequency range on E-Plane. The total directivity can be improved by adding more sub-arrays and photodiodes.

V. Conclusion and Perspectives

This paper presents the design of a photonically excited phased array capable of steering in a $\pm 30°$ angular range on E-plane. The complexity of this configuration arises from the challenge of achieving the desired radiation characteristics with a substrate possessing low permittivity and losses in the mm-wave range, while including the elements required for biasing the photodiodes in the InP chip. Hence, the inclusion of vias to obtain a compact shorted patch has been implemented as a solution. One can observe that the directivity is somehow limited, which stems from the fact that the phased array consists of only four sub-arrays counting 2 radiating elements each for a total of 8 radiating elements. As we discussed, this can be solved by adding more radiation elements and consequently adding more photodiodes, something that will increase the gain and the total emitted power.

Acknowledgment

This work has received support from the French Government through the Labex CominLabs Excellence Laboratory, managed by ANR in the Investing for the Future Program under Reference ANR-10-LABX-07-01 and the European Union through European Regional Development Fund (ERDF), Ministry of Higher Education and Research, CNRS, Brittany region, Conseils Départementaux d'Ille-et-Vilaine and Côtes d'Armor, Rennes Métropole, and Lannion Trégor Communauté, through the CPER Projects CyMoCod and Phot-Breizh. Also we would like to thank Frédéric van Dijk from III-V Lab for useful discussions.

References

[1] "Ericsson Mobility Report", no. June, 2023 .
[2] F. Tariq, M. R. A. Khandaker, K. K. Wong, M. A. Imran, M. Bennis, and M. Debbah, "A Speculative Study on 6G," *IEEE Wireless Commun.*, vol. 27, no. 4, pp. 118–125, Aug. 2020.
[3] T. Nagatsuma, G. Ducournau, and C. C. Renaud, "Advances in terahertz communications accelerated by photonics," Nature Photon, vol. 10, no. 6, pp. 371–379, Jun. 2016.
[4] A. Pärssinen *et al.*, *White paper on RF enabling 6G: opportunities and challenges from technology to spectrum*, 6G Research Visions, No. 13 University of Oulu, 2021, pp.9-16.
[5] Ali, M. *et al.*, "Antenna Arrays for Beamforming," in *THz Communications: Paving the Way Towards Wireless Tbps*, T. Kürner, D. M. Mittleman, and T. Nagatsuma, Eds., Cham: Springer International Publishing, 2022, pp. 161–174.
[6] Á. J. Pascual et al., "Photonic-Enabled Beam Switching Mm-Wave Antenna Array," *J. Lightw. Technol.*, vol. 40, no. 3, pp. 632–639, Feb. 2022.
[7] J.-S. Kuo and K.-L. Wong, "A low-cost microstrip-line-fed shorted-patch antenna for a PCS base station," *Microw. Opt. Technol. Lett.*, vol. 29, no. 3, pp. 146–148, 2001.
[8] A. Rolland, G. Loas, M. Brunel, L. Frein, M. Vallet, and M. Alouini, "Non-linear optoelectronic phase-locked loop for stabilization of opto-millimeter waves: towards a narrow linewidth tunable THz source," *Opt. Express*, OE, vol. 19, no. 19, pp. 17944–17950, Sep. 2011.
[9] G. Danion, C. Hamel, L. Frein, F. Bondu, G. Loas, and M. Alouini, "Dual frequency laser with two continuously and widely tunable frequencies for optical referencing of GHz to THz beatnotes," *Opt. Express*, OE, vol. 22, no. 15, pp. 17673–17678, Jul. 2014.
[10] H.-J. Song, K. Ajito, Y. Muramoto, A. Wakatsuki, T. Nagatsuma, and N. Kukutsu, "Uni-Travelling-Carrier Photodiode Module Generating 300 GHz Power Greater Than 1 mW," *IEEE Microw. and Wireless Comp. Lett.*, vol. 22, no. 7, pp. 363–365, Jul. 2012.
[11] Á. J. Pascual-Gracia *et al.*, "A Photonically-Excited Leaky-Wave Antenna Array at E-Band for 1-D Beam Steering," *Appl. Sci.*, vol. 10, no. 10, p. 3474, May 2020.
[12] I. Huynen and G. Dambrine, "A novel CPW DC-blocking topology with improved matching at W-band," *IEEE Microw. Guid. Wave Lett.*, vol. 8, no. 4, pp. 149–151, April 1998.
[13] B.-K. Tan and G. Yassin, "A Slotline DC Block for Microwave, Millimetre and Sub-Millimetre Circuits," *IEEE Microw. Wireless Compon. Lett.*, 2019.
[14] E. Rouvalis *et al.*, "High-speed photodiodes for InP-based photonic integrated", *IEEE Photon. Conf. IPC*, vol. 20, no. 8, pp. 88-89, 2012.